the metal d_{yz} orbitals. Linear combinations of $1a_u$ and $3b_g$ can be made in order to emphasize net interactions. Orbitals $1a_g$, $4b_u$, $5a_g$, and the linear combinations of $1a_u$ and $3b_g$ are shown in Figure 5. Of course $1a_u$ and $3b_g$ can be regenerated by adding or subtracting, respectively, the linear combinations illustrated in Figure 5.

According to the 18-electron rule, the formal metal–metal bond orders of the dicarbonyl- and dinitrosyl-bridged dimers are 2.0 and 1.0, respectively. In the dicarbonyl-bridged dimers all orbitals shown in Figure 5 are filled except $5a_g$, the LUMO. The two metal–metal bonds are represented by $1a_g$ and $4b_u$. These are 4c–2e bonds and contain substantial amounts of CpM–EO bonding. The linear combinations of $1a_u$ and $3b_g$ are exclusively CpM–EO bonding. In dinitrosyl-bridged dimers all orbitals are filled, including $5a_g$. The out-of-plane π metal–metal bond in $4b_u$ is more than cancelled by the out-of-plane π^* metal–metal antibond in $5a_g$. Therefore, in dinitrosyl-bridged dimers the only net metal–metal bonding interaction is the in-plane σ bond in $1a_g$. The description given above neglects the $1e_2$ and $1a_1$ fragment orbitals and this t_{2g}-like set is usually believed not to contribute to metal–metal bonding, but as shown in Table VI and in Figure 4, the $1a_1$ fragment orbitals do contribute some additional metal–metal bonding because the bonding in the $3a_g$ is not completely cancelled by their antibonding counterpart, $3b_u$.

Acknowledgment. We thank the Robert A. Welch Foundation (Grant No. A-648) for the support of this work and the National Science Foundation for funds to purchase the VAX 11/780 (Grant No. CHE80-15792). We also thank Professor William A. G. Graham of the University of Alberta for his generous gift of $Cp^*_2Ir_2(CO)_2$.

Registry No. $Cp^*_2Co_2(CO)_2$, 69657-52-9; $Cp^*_2Rh_2(CO)_2$, 69728-34-3; $Cp_2Co_2(NO)_2$, 51862-20-5; $Cp_2Rh(NO)_2$, 67426-08-8; $Cp^*_2Ir(CO)_2$, 106682-38-6.

Low-Valent Rhenium–Oxo–Alkoxide Complexes: Synthesis, Characterization, Structure, and Ligand Exchange and Carbon Monoxide Insertion Reactions[1]

Torsten K. G. Erikson, Jeffrey C. Bryan, and James M. Mayer*

Department of Chemistry, University of Washington, Seattle, Washington 98195

Received October 2, 1987

A series of rhenium(III)–oxo–alkoxide–bis(acetylene) complexes of the form $Re(O)(OR)(R'C{\equiv}CR')_2$ have been prepared by reaction of the iodide derivatives $Re(O)I(R'C{\equiv}CR')_2$ with thallium alkoxides. An X-ray crystal structure of the phenoxide complex **7a** shows the pseudotetrahedral coordination geometry typical of $Re(O)X(RC{\equiv}CR)_2$ compounds, with a short rhenium–oxo bond of 1.712 (13) Å and a longer Re–OPh distance of 1.966 (14) Å. The alkoxide complexes decompose in solution at less than 100 °C by a number of pathways including β-hydrogen elimination. The complexes react rapidly with protic reagents such as alcohols, water, amines, acids, etc. with displacement of alcohol. Reactions of the *tert*-butoxide complex with ammonia or methylamine yield the corresponding amide complexes, and H_2S gives the hydrosulfide species. Many of these ligand exchange reactions give equilibrium mixtures, indicating that the Re–X bond strengths in general parallel H–X bond strengths. The methylamide complex is fluxional on the NMR time scale, with a ground state that places the methyl group pointing at one of the acetylene ligands. The phenoxide ligand in the X-ray structure is approximately in the same sterically encumbered orientation. This orientation is preferred because it favors π-bonding and minimizes π-antibonding interactions of the π-donor orbital of the amide or phenoxide ligand. The ethoxide complex readily inserts carbon monoxide and isopropyl isocyanide to give $Re(O)[C(O)OEt](MeC{\equiv}CMe)_2$ and $Re(O)[C(N\text{-}i\text{-}Pr)OEt](MeC{\equiv}CMe)_2$, respectively. Crystal data for **7a**: $Pna2_1$, a = 18.620 (7) Å, b = 7.2389 (9) Å, c = 10.552 (3) Å, Z = 4, refined to R = 0.044, R_w = 0.044.

We have been studying the chemistry of low-valent rhenium–oxo compounds since our discovery of $Re(O)I(MeC{\equiv}CMe)_2$ (**1a**) in 1984.[2] This compound and its derivatives are remarkable because they contain terminal oxo groups with strong metal–oxygen multiple bonds despite a low formal oxidation state (+3) and a d^4 electron count.[3-5] Compounds with terminal oxo ligands almost always have high oxidation states and d^0, d^1, or d^2 electronic configurations.[6] Previous papers in this series have presented a description of the electronic structure of d^4 oxo–acetylene compounds,[3] discussed their ligand substitution reactions,[7] and described their reduction to di-

(1) Low-Valent Oxo Compounds. 5. For previous papers in this series see ref 2, 3, 7, and 8.
(2) Mayer, J. M.; Tulip, T. H. *J. Am. Chem. Soc.* **1984**, *106*, 3878–9.
(3) Mayer, J. M.; Thorn, D. L.; Tulip, T. H. *J. Am. Chem. Soc.* **1985**, *107*, 7454–7462.
(4) Another d^4 rhenium–oxo compound has recently been described: de Boer, E. J. M.; de With, J.; Orpen, A. G. *J. Am. Chem. Soc.* **1986**, *108*, 8271–3.
(5) For other terminal oxo complexes in d^3 or d^4 configurations, see: Meyer, T. J. et al. *Inorg. Chem.* **1981**, *20*, 436–444; **1983**, *22*, 1407–9; **1984**, *23*, 1845–1851; **1986**, *25*, 3256–3262; *J. Am. Chem. Soc.* **1986**, *108*, 4066–4073. Marmion, M. E.; Takeuchi, K. J. *J. Am. Chem. Soc.* **1986**, *108*, 510–511. Che, C.-M.; Lai, T.-F.; Wong, K.-Y. *Inorg. Chem.* **1987**, *26*, 2289–2299. Aoyagi, K.; Yukawa, Y.; Shimizu, K.; Mukaida, M.; Takeuchi, T.; Kakihana, H. *Bull. Chem. Soc. Jpn.* **1986**, *59*, 1493–1499.
(6) Nugent, W. A.; Mayer, J. M. *Metal.-Ligand Multiple Bonds*; Wiley: New York, in press. Griffith, W. P. *Coord. Chem. Rev.* **1970**, *5*, 459–517.

0276-7333/88/2307-1930$01.50/0

Scheme I

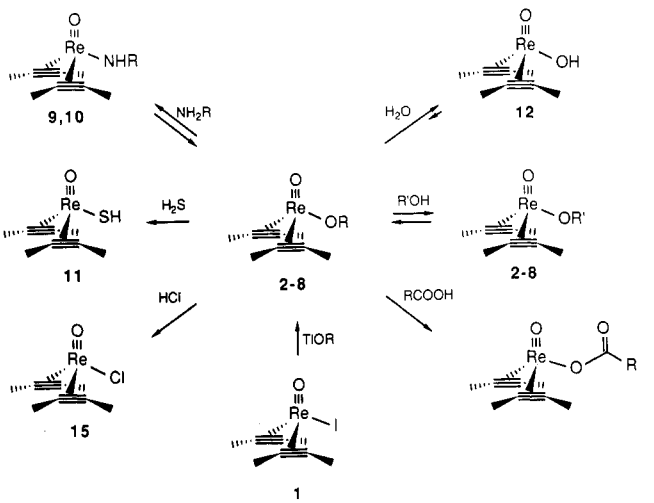

mers of the form $Re_2(O)_2(RC{\equiv}CR)_4$.[8] In this report we describe the synthesis and characterization of molecules with alkoxide, amide, and hydrosulfide ligands bound to the $Re(O)(RC{\equiv}CR)_2$ fragment. These π-donor ligands provide a probe of the electronic structure of the molecules, and they are the primary site of reactivity including ligand exchange reactions and CO insertion. The chemistry of the related rhenium-oxo-hydroxide complex $Re(O)(OH)(RC{\equiv}CR)_2$, in particular its proton-transfer reactions, are discussed in an upcoming report.[9]

Results

Rhenium(III)-oxo-alkoxide complexes are prepared by treatment of $Re(O)I(MeC{\equiv}CMe)_2$ (**1a**), $Re(O)I(EtC{\equiv}CEt)_2$ (**1b**), or $Re(O)I(t\text{-}BuC{\equiv}CH)_2$ (**1c**)[3] with a slight excess of the appropriate thallium alkoxide[10] (eq 1; Scheme I). After removal of TlI by filtration, the products are isolated by sublimation (30–50 °C, 10^{-3} mmHg) in 60–80% yields as yellow-green crystalline solids. The phenoxide **7a** is stable to air for days, but the other compounds are more reactive: **3a** decomposes within seconds of exposure to air. Control of the reaction stoichiometry is important because the use of excess thallium alkoxide leads to oily products that do not sublime cleanly. Reactions with alkali-metal alkoxides instead of thallium reagents require longer reaction times and give lower yields.

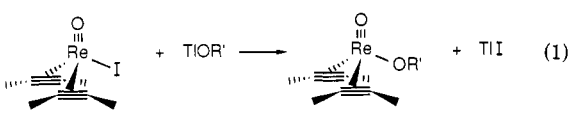

$Re(O)(OR')(MeC{\equiv}CMe)_2$: R' = Me (**2a**), Et (**3a**), *i*-Pr (**4a**), *t*-Bu (**5a**), $OSiMe_3$ (**6a**), Ph (**7a**), $CH_2CH{=}CH_2$ (**8a**)
$Re(O)(OR')(EtC{\equiv}CEt)_2$: R' = Me (**2b**), Et (**3b**)
$Re(O)(OR')(^tBuC{\equiv}CH)_2$: R' = Et (**3c**), Ph (**7c**)

Corresponding amide complexes are prepared by displacement of the *tert*-butoxide ligand in **5a** with ammonia or methylamine (Scheme I; eq 2). Compounds **9a** and **10a** are isolated in ~55% yields after sublimation at 40–50 °C in vacuo, **9a** as a beige-white powder and **10a** as a pale yellow-green crystalline solid. The related reaction of H_2S with **3a** forms ethanol and the hydrosulfide complex **11a**, isolated as a colorless solid in 90% yield after sublimation (eq 3). The oxo-hydroxide complexes $Re(O)(OH)(R'C{\equiv}CR')_2$ (**12a** and **12b**) are prepared similarly by hydrolysis of **3a**.[9] Attempts to prepare the amide complexes from the ethoxide **3a** yielded only equilibrium mixtures of **3a** and **9a** or **10a** (see below).

$$\underset{\textbf{5a}}{Re(O)(O\text{-}t\text{-}Bu)(MeC{\equiv}CMe)_2} + NH_2R \rightarrow \underset{\textbf{9a, R = H}\\ \textbf{10a, R = Me}}{Re(O)(NHR)(MeC{\equiv}CMe)_2} + t\text{-}BuOH \quad (2)$$

$$\underset{\textbf{3a}}{Re(O)(OEt)(MeC{\equiv}CMe)_2} + H_2S \rightarrow \underset{\textbf{11a}}{Re(O)(SH)(MeC{\equiv}CMe)_2} + EtOH \quad (3)$$

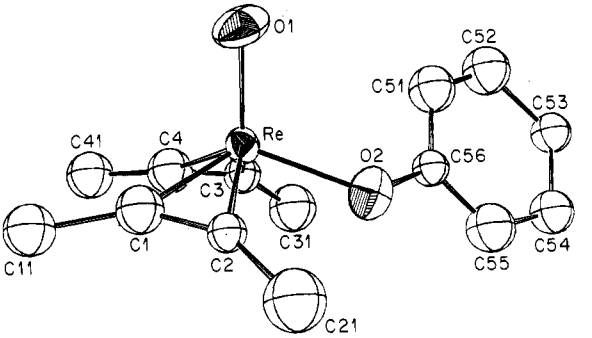

Figure 1. ORTEP drawing of $Re(O)(OPh)(MeC{\equiv}CMe)_2$ (**7a**) with hydrogen atoms omitted for clarity.

The oxo-alkoxide, -amide, and -hydrosulfide compounds have been characterized by IR and NMR spectroscopies, by the observation of parent ions in their mass spectra, and in the case of **7a** by an X-ray crystal structure. Compounds **3a**, **9a**, **10a**, and **11a** have been found to be monomeric in methylene chloride solution. The IR spectra all contain a strong band in the region 935–970 cm^{-1}, signifying the presence of an Re≡O unit. This assignment has been confirmed by the expected shift on oxygen-18 substitution of the terminal oxo in **3a** ($\nu(ReO)$ = 964, $\nu(Re^{18}O)$ = 916 cm^{-1}). The amide complexes exhibit the lowest Re≡O stretching frequencies, at 945 (**9a**) and 936 cm^{-1} (**10a**). The acetylene ligands give rise to symmetric and antisymmetric stretching modes of low intensity (~1815 and 1760 cm^{-1} for the 2-butyne derivatives). The alkoxide complexes exhibit bands in the regions 500–610 and 1000–1200 cm^{-1} assigned to Re–OR and O–C stretching modes, by analogy to d^1 and d^2 alkoxide complexes of molybdenum and tungsten.[11] The assignments are also consistent with the ^{18}O- and ^2H-labeling study of the oxo-hydroxide complex.[9] The amide derivatives show characteristic N–H stretches (**9a**, 3463 and 3371 cm^{-1}, **10a**, 3486 cm^{-1}) and the S–H absorption in **11a** is found at 2547 cm^{-1}.[12]

The NMR spectra of **2**–**11** are very similar to those of the iodide starting materials, with additional resonances for the alkoxide, amide, or SH ligands. Two resonances are observed for the four acetylene substituents in the 2-butyne and 3-hexyne complexes, consistent with the pentagonal-pyramid geometry found for **1a**[3] and **7a** in the solid state (Figure 1). The ^{13}C chemical shifts for the acetylenic carbons of the alkoxide derivatives **2a**–**8a** (δ ~145, 155) are close to those of **1a**[3] (δ 138, 142).

(7) Mayer, J. M.; Tulip, T. H.; Calabrese, J. C.; Valencia, E. *J. Am. Chem. Soc.* **1987**, *109*, 157–163.
(8) Valencia, E.; Santarsiero, B. D.; Geib, S. J.; Rheingold, A. L.; Mayer, J. M. *J. Am. Chem. Soc.* **1987**, *109*, 6896–8.
(9) Erikson, T. K. G.; Mayer, J. M., submitted for publication in *Angew. Chem.*
(10) Lee, A. G. *The Chemistry of Thallium*; Elsevier: New York, 1971.
(11) Reagan, W. J.; Brubaker, C. H., Jr. *Inorg. Chem.* **1970**, *9*, 827–830. Rillema, D. P.; Brubaker, C. H., Jr. *Ibid.* **1969**, *8*, 1645–9. Rillema, D. P.; Reagan, W. J.; Brubaker, C. H. Jr. *Ibid.* **1969**, *8*, 587–590.
(12) Compare other M–SH compounds: 2580 cm^{-1} in $Cp^*_2Ti(SH)_2$, Bottomley, F.; Drummond, D. F.; Egharevba, G. O.; White, P. S. *Organometallics* **1986**, *5*, 1620–5; 2508 cm^{-1} in $Cp^*(PMe_3)_2Ru(SH)$, ref 26.

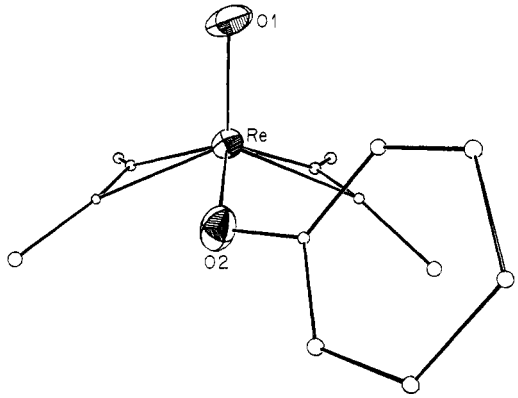

Figure 2. ORTEP drawing of Re(O)(OPh)(MeC≡CMe)$_2$ (**7a**) with carbon atoms drawn as small spheres and with hydrogen atoms omitted.

Table I. Positional and Equivalent Isotropic Thermal Parameters for Re(O)(OPh)(MeC≡CMe)$_2$ (7a)[a]

atom	*x*	*y*	*z*	*B*
Re	0.87817 (2)	0.94533 (6)	1.000	2.210 (8)
O(1)	0.9072 (8)	1.038 (2)	1.140 (1)	4.2 (3)
O(2)	0.8082 (7)	1.112 (2)	0.920 (1)	3.5 (2)
C(1)	0.967 (1)	0.886 (3)	0.897 (1)	3.2 (3)*
C(2)	0.9371 (8)	1.029 (2)	0.849 (1)	2.2 (3)*
C(3)	0.8000 (8)	0.744 (2)	1.020 (1)	2.6 (3)*
C(4)	0.8623 (9)	0.677 (2)	1.022 (2)	4.0 (3)*
C(11)	1.023 (1)	0.746 (3)	0.879 (2)	4.3 (4)*
C(21)	0.935 (1)	1.175 (3)	0.748 (2)	4.4 (4)*
C(31)	0.722 (1)	0.711 (3)	1.010 (3)	6.2 (4)*
C(41)	0.896 (1)	0.494 (4)	1.041 (2)	4.8 (4)*
C(51)	0.723 (1)	1.151 (3)	1.095 (2)	4.3 (4)*
C(52)	0.652 (1)	1.202 (4)	1.135 (2)	6.2 (6)*
C(53)	0.603 (1)	1.245 (3)	1.039 (1)	3.4 (4)*
C(54)	0.6163 (9)	1.240 (3)	0.915 (2)	3.4 (3)*
C(55)	0.684 (1)	1.188 (2)	0.880 (1)	3.2 (3)*
C(56)	0.740 (1)	1.146 (2)	0.966 (1)	2.3 (3)*

[a] Parameters with an asterisk refined isotropically. *B* values (Å^2) for anisotropically refined atoms are given in the form of the equivalent isotropic thermal parameter defined as $^4/_3[a^2B(1,1) + b^2B(2,2) + c^2B(3,3) + ab(\cos\gamma)B(1,2) + ac(\cos\beta)B(1,3) + bc(\cos\alpha)B(2,3)]$.

Complex **10a** exhibits restricted rotation of the methyl–amide ligand on the NMR time scale: at −40 °C the ^{13}C NMR spectrum shows four different acetylenic carbons which coalesce into two broad signals at 25 °C. The low-temperature conformation of **10a** must therefore have the methyl of the amide ligand pointing at one of the acetylenes, as shown in A. This conformation appears to be

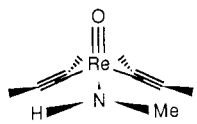

A

more sterically hindered than one where the methyl points away from the oxo and is probably favored for an electronic reason (see Discussion). From the coalescence of methyl resonances in the ^{1}H NMR at −19 °C, the rate of amide rotation is found to be $k = 2.6\ (\pm 0.8) \times 10^2\ s^{-1}$, corresponding to a free energy of activation of $\Delta G^{\ddagger} = 12.0 \pm 0.2$ kcal/mol.

Crystals of **7a** were grown by slow evaporation of a pentane solution and fully characterized by an X-ray crystal structure (Figures 1 and 2). Fractional atomic coordinates are given in Table I, and relevant bond distances and angles are given in Table II. The ligating

Table II. Selected Bond Lengths and Angles (deg) in Re(O)(OPh)(MeC≡CMe)$_2$ (7a)

Bond Lengths			
Re–O(1)	1.712 (13)	C(1)–C(2)	1.27 (3)
Re–O(2)	1.966 (14)	C(1)–C(11)	1.47 (3)
Re–C(1)	2.02 (2)	C(2)–C(21)	1.51 (3)
Re–C(2)	2.02 (2)	C(3)–C(4)	1.26 (2)
Re–C(3)	2.07 (2)	C(3)–C(31)	1.47 (3)
Re–C(4)	1.98 (2)	C(4)–C(41)	1.48 (4)
		O(2)–C(56)	1.38 (2)
Bond Angles			
O(1)–Re–O(2)	109.9 (7)	C(2)–C(1)–C(11)	145 (2)
O(1)–Re–C(1)	106.9 (8)	Re–C(2)–C(1)	71.6 (12)
O(1)–Re–C(2)	113.0 (7)	Re–C(2)–C(21)	139 (2)
O(1)–Re–C(3)	114.1 (8)	C(1)–C(2)–C(21)	149 (2)
O(1)–Re–C(4)	109.3 (9)	Re–C(3)–C(4)	68.0 (11)
O(2)–Re–C(1)	116.0 (7)	Re–C(3)–C(31)	143 (2)
O(2)–Re–C(2)	80.7 (6)	C(4)–C(3)–C(31)	148 (2)
O(2)–Re–C(3)	90.6 (7)	Re–C(4)–C(3)	75.9 (11)
O(2)–Re–C(4)	123.6 (8)	Re–C(4)–C(41)	146 (2)
C(1)–Re–C(2)	36.6 (9)	C(3)–C(4)–C(41)	138 (2)
C(1)–Re–C(4)	88.8 (9)	O(2)–C(56)–C(51)	124 (2)
C(2)–Re–C(3)	132.2 (8)	O(2)–C(56)–C(55)	119.6 (13)
C(3)–Re–C(4)	36.1 (7)	C(51)–C(56)–C(55)	117 (2)
Re–O(2)–C(56)	124.5 (11)		
Re–C(1)–C(2)	71.8 (12)		
Re–C(1)–C(11)	143 (2)		

atoms define an approximate pentagonal pyramid about the rhenium center, with the oxo group at the apex. Alternatively the coordination geometry can be described as roughly tetrahedral with the acetylene midpoints occupying two of the vertices. The overall configuration and the metrical data are quite similar to the structures of **1a**,[3] Re(O)(Et)(MeC≡CMe)$_2$,[13] [Re(O)(MeC≡CMe)$_2$L]SbF$_6$ (L = py, bpy),[7] and [Re(O)(MeC≡CMe)$_2$]$_2$.[8] The rhenium–oxo bond length in **7a** of 1.712 (13) Å is typical of the distances found in the complexes above. The rhenium–phenoxide bond length of 1.966 (14) Å lies in the middle of the range of reported Re–alkoxide distances, from less than 1.9 Å for alkoxides that are strongly engaged in π-bonding (e.g., Re(O)(OEt)Cl$_2$(py)$_2$, 1.896 (6) Å[14]) to >2.0 Å for those that are not (e.g., Re$_2$Cl$_5$(OEt)(dppm)$_2$, 2.085 (14) Å[15]).[16] The small Re–O(2)–C(56) angle of 124.5 (11)° also indicates that rhenium–phenoxide π-bonding is not a dominant interaction.[17]

The coordination geometry of the phenoxide complex **7a** differs from the iodide, ethyl, pyridine, and bipyridine derivatives because **7a** does not have a pseudo-mirror plane that relates the two acetylene ligands. The phenoxide ligand does not point away from the oxo group as might be expected on steric grounds and as found for the ethyl

(13) Spaltenstein, E.; Erikson, T. K. G.; Critchlow, S. C.; Mayer, J. M., submitted for publication in *J. Am. Chem. Soc.*

(14) Lock, C. J. L.; Turner, G. *Can. J. Chem.* **1977**, *55*, 333–9.

(15) Barder, T. J.; Cotton, F. A.; Lewis, D.; Schwotzer, W.; Tetrick, S. M.; Walton, R. A. *J. Am. Chem. Soc.* **1984**, *106*, 2882–2891.

(16) Other rhenium alkoxide/phenoxide structures: Edwards, P. G.; Wilkinson, G.; Hursthouse, M. B.; Malik, K. M. A. *J. Chem. Soc., Dalton Trans.* **1980**, 2467–2475. Chakravarty, A. R.; Cotton, F. A.; Cutler, A. R.; Walton, R. A. *Inorg. Chem.* **1986**, *25*, 3619–3624.

(17) Discussions of metal–alkoxide and –phenoxide bonding can be found in the following and in ref 18 and 23. Fanwick, P. E.; Ogilvy, A. E.; Rothwell, I. P. *Organometallics* **1987**, *6*, 73–80 and references therein. LaPointe, R. E.; Wolczanski, P. T., Mitchell, J. F. *J. Am. Chem. Soc.* **1986**, *108*, 6382–6384. Coffindaffer, T. W.; Rothwell, I. P.; Huffman, J. C. *Inorg. Chem.* **1983**, *22*, 2906–2910 and references therein. Kamenar, B.; Penavic, M. *J. Chem. Soc.*, Dalton *Trans.* **1977**, 356–8. Chisholm, M. H.; Eichhorn, B. W.; Folting, K.; Huffman, J. C.; Tatz, R. J. *Organometallics* **1986**, *5*, 1599–1606 and ref therein. Davies, J. I.; Gibson, J. F.; Skapski, A. C.; Wilkinson, G.; Wong, W.-K. *Polyhedron* **1982**, *1*, 641–6. Chiu, K. W.; Jones, R. A.; Wilkinson, G.; Galas, A. M. R.; Hursthouse, M. B.; Malik, K. M. A. *J. Chem. Soc., Dalton Trans.* **1981**, 1204–1211.

(18) Bryndza, H. E.; Calabrese, J. C.; Marsi, M.; Roe, D. C.; Tam, W.; Bercaw, J. E. *J. Am. Chem. Soc.* **1986**, *108*, 4805–4813.

complex.[13] Rather the phenoxide is oriented toward one of the acetylene ligands (Figure 2) as indicated by the torsion angle O(1)–Re–O(2)–C(56) of 69.2 (14)°. This is close to the conformation proposed for the methylamide complex **10a** on the basis of NMR spectra (see A above). The phenoxide oxygen lies substantially closer to C(2) than C(3) (∠O(2)–Re–C(2) = 80.7 (6)°; O(2)–Re–C(3) = 90.6 (7)°), with a short contact between O(2) and C(2) of 2.58 Å (compare O(2)···C(3) = 2.87 Å; the sum of the van der Walls radii of carbon and oxygen is ~3.1 Å[19]). There is also a close contact between one of the acetylenic carbons and the ipso carbon of the phenyl ring, C(3)···C(56) = 3.17 Å. The conformation of the phenoxide does not appear to be due to intermolecular interactions in the crystal (such as phenyl ring stacking), rather this orientation is favored by electronic factors (see Discussion).

The oxo–alkoxide compounds **2–8** are less thermally stable than the analogous halide or alkyl complexes, decomposing in benzene solution at temperatures lower than 100 °C. The ethoxide **3a**, for example, decomposes over 2 days at 70 °C to give a mixture of products including the rhenium–oxo–hydride $Re(O)H(MeC{\equiv}CMe)_2$ (**13a**),[13] the rhenium(II)–oxo dimer $[Re(O)(MeC{\equiv}CMe)_2]_2$ (**14a**),[8] ethanol, 2-butyne, acetaldehyde, hexamethylbenzene, etc. The formation of the hydride **13a** and acetaldehyde in equimolar quantities (~10% yield from **3a**, 25% yield of **13b** from **3b**) suggests that β-hydrogen elimination from the ethoxide ligand[20] is one of the decomposition pathways, although not a predominant one. The hydride complex **13a** is also formed in the decompositions of **2a** and **4a** but not on heating the *tert*-butoxide and phenoxide derivatives (**5** and **7a**) which do not have β-hydrogen atoms in the alkoxide ligand. The observation of β-hydrogen elimination from alkoxide ligands is surprising since related alkyl complexes do not β-hydrogen eliminate even for extended periods at 120 °C.[13]

The ethoxide complex **3a** reacts in chloroform-d_1 solvent at 70 °C to give the rhenium–chloride derivative $Re(O)Cl(MeC{\equiv}CMe)_2$ (**15a**)[3] in 60% yield (eq 4) together with

$$\underset{\mathbf{3a}}{Re(O)(OEt)(MeC{\equiv}CMe)_2} + CDCl_3 \rightarrow \underset{\mathbf{15a}}{Re(O)Cl(MeC{\equiv}CMe)_2} + \ldots \quad (4)$$

$CHDCl_2$ and the organic products listed above. The chloride complex **15a** is also formed on reaction of chloroform with **5a** and **7a**. Methyl iodide reacts very slowly with **3a** giving a mixture of products with only a small amount of **1a**. Complex **3a** does not react with carbon dioxide, ethylene, or dihydrogen before decomposition.

The oxo–alkoxide complexes react rapidly at ambient temperatures with protic reagents—alcohols, water, acetic acid, amines, HCl, and H_2S—by exchange of the alkoxide for another ligand (Scheme I). This reaction has been used to prepare compounds **9a–11a** (eq 2 and 3). In many cases an equilibrium is established with significant quantities of both the starting alkoxide complex and the product; these reactions can be driven in either direction by the presence of excess protic reagent. The equilibrium constants for these reactions in benzene-d_6 solution have been determined by integration of ^1H NMR spectra and are listed in Table III along with calculated free energies. The reactions of **3a** with HCl, acetic acid, H_2O, and H_2S appear to proceed to completion even in the presence of only 1 equiv of reagent. Dimethylamine and *tert*-butyl alcohol do not react with **3a** presumably because of the steric bulk of these ligands.

Table III. Ligand Exchange Reactions: Equilibrium Constants and Free Energy Differences[a]

$$Re(O)(X)(MeC{\equiv}CMe)_2 + HY \rightleftharpoons Re(O)(Y)(MeC{\equiv}CMe)_2 + HX$$

X	Y	K_{eq}	ΔG_{eq}[b]	rel D-(Re–X)$_{soln}$[b,c]
OEt	OEt	1	0	0
OEt	OMe	0.8	0.1 ± 0.2	0.1
OEt	O-*i*-Pr	0.9	0.06 ± 0.1	0.4
OEt	O-*t*-Bu	$<6 \times 10^{-3}$	>3.0	<-2.8
OEt	OPh	$>2 \times 10^{3}$	<-4.5	<-11.7
OEt	OH	$>1.2 \times 10^{2}$	<-2.8	>17.4
OEt	OAc[d]	$>6 \times 10^{5}$ [d]	<-6.8	>15.7
OEt	NH_2	7.4	-1.2 ± 0.2	7.0
OEt	NHMe	0.6	0.3 ± 0.2	-1.5
OEt	NHEt	0.4	0.5 ± 0.2	-3.7
OEt	NMe_2	$<5 \times 10^{-4}$	>4.5	<-14.4
OEt	Cl	$>1 \times 10^{4}$	<-5.5	>4.5
OEt	SH	$>4 \times 10^{4}$	<-6.3	>-2.1
NH_2	OPh	37	-2.1 ± 0.2	20
NH_2	OH	11	-1.4 ± 0.2	-10.4
OH	OPh	18	-1.7 ± 0.2	29
SH	OH	$<1 \times 10^{-4}$	>5.5	>-24
SH	OAc	$<9 \times 10^{-4}$	>4.2	>-17.8
OH	OAc	$>5 \times 10^{3}$	<-5.0	<2.0
O-*t*-Bu	NMe_2	8.5×10^{-2}	1.5 ± 0.2	11.6
NHMe	OH	$>2 \times 10^{2}$	<-3.1	<-19.1
O-*t*-Bu	NHMe	$>3 \times 10^{2}$	<-3.4	<-1.3

[a] Determined in C_6D_6 solvent at 22 ± 2 °C. [b] In kcal/mol. [c] Bond strength relative to Re–OEt, in kcal/mol, following ref 26. [d] Calculated from K_{eq} for Re–OEt + H_2O and for Re–OH + HOAc.

The rate of reaction of the alkoxide compounds with alcohol is fast on the chemical time scale (within minutes of mixing) but slow on the NMR time scale even at 100 °C. Thus solutions of **3a** and ethanol (eq 5) show separate resonances in the ^1H NMR for the ethoxide and EtOH groups. Addition of 0.1 equiv of acetic acid results in

$$\underset{\mathbf{3a}}{Re(O)(OEt)(MeC{\equiv}CMe)_2} + *EtOH \rightleftharpoons \underset{\mathbf{3a}}{Re(O)(O*Et)(MeC{\equiv}CMe)_2} + EtOH \quad (5)$$

coalescence of the ethyl group signals, indicating that the weak acid catalyzes the ligand exchange. In contrast, bases such as LiO-*t*-Bu or "Proton Sponge" (1,8-bis(dimethylamino)naphthalene) have little effect on reaction 5. The resonances for the acetylene substituents remain sharp even under conditions where alkoxide exchange is rapid. The ethoxide ligand in **3a** will also exchange with an alkoxy group bound to another rhenium center: a mixture of **3a** and **2b** in benzene within 24 h forms an equimolar equilibrium mixture of **3a**, **3b**, **2a**, and **2b** (eq 6).

$$\underset{\mathbf{3a}}{Re(O)(OEt)(MeC{\equiv}CMe)_2} + \underset{\mathbf{2b}}{Re(O)(OMe)(EtC{\equiv}CEt)_2} \rightleftharpoons \underset{\mathbf{2a}}{Re(O)(OMe)(MeC{\equiv}CMe)_2} + \underset{\mathbf{3b}}{Re(O)(OEt)(EtC{\equiv}CEt)_2} \quad (6)$$

The ethoxide complex **3a** reacts with carbon monoxide under mild conditions (1 atm, 25 °C, 3 days) to give the ethoxycarbonyl complex **16a** in 45% yield after sublimation (eq 7). Sublimation separates **16a** from other

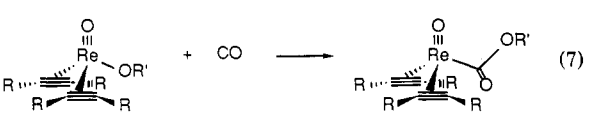

(7)

(19) Huheey, J. E. *Inorganic Chemistry*; Harper & Row: New York, 1972; p 184.

(20) For other examples of β-hydrogen elimination from alkoxide ligands, see ref 18 and references therein and: Vaska, L.; diLuzio, J. W. *J. Am. Chem. Soc.* **1962**, *84*, 4989–4990. Bernard, K. A.; Rees, W. M.; Atwood, J. D. *Organometallics* **1986**, *5*, 390–1.

product(s) of the carbonylation reaction, believed to be rhenium carbonyl species because of several bands observed in the IR spectrum in the region 2100–1900 cm^{-1}. Analogous reactions of **2a**, **2b**, **3b**, **5a**, and **8a** have been observed (by NMR and IR), but **7a** does not react with CO over 1 day at 70 °C. This reaction contrasts with the lack of CO insertion into the related alkyl complexes such as $Re(O)Et(MeC{\equiv}CMe)_2$.[13] Isopropyl isocyanide also inserts into the ethoxide ligand of **3a**; a 38% isolated yield of **17a** was obtained after sublimation (eq 8). The hydroxide

$$\underset{\textbf{3a}}{Re(O)(OEt)(MeC{\equiv}CMe)_2} + CN\text{-}i\text{-}Pr \rightarrow \underset{\textbf{17a}}{Re(O)[C(N\text{-}i\text{-}Pr)OEt](MeC{\equiv}CMe)_2} \quad (8)$$

complex **12a** reacts with CO but does not give a hydroxycarbonyl complex (ReC(O)OH), forming instead the rhenium(II) dimer **14a**,[8] CO_2, and water (eq 9)

$$\underset{\textbf{12a}}{Re(O)(OH)(MeC{\equiv}CMe)_2} + CO \rightarrow \underset{\textbf{14a}}{[Re(O)(MeC{\equiv}CMe)_2]_2} + CO_2 + H_2O + \ldots \quad (9)$$

The alkoxycarbonyl complexes appear to have the same basic structure as the alkoxide compounds on the basis of NMR and IR spectra. Two sets of acetylene substituents are observed for the $Re(O)(RC{\equiv}CR)_2$ fragment, and the acetylenic carbon atoms appear at $\delta \sim 140$ in the ^{13}C NMR. The carbonyl carbon is found at δ 204 and the C=O stretching frequency is approximately 1660 cm^{-1}, similar to the values found for other examples of this ligand.[21-23]

The ethoxycarbonyl **16a** can be converted to the methoxy derivative by heating with excess methanol for 10 h at 70 °C (eq 10). The conditions of this reaction contrast

$$\underset{\textbf{16a}}{Re(O)[C(O)OEt](MeC{\equiv}CMe)_2} + MeOH \rightarrow Re(O)[C(O)OMe](MeC{\equiv}CMe)_2 + EtOH \quad (10)$$

with the facile exchange of alkoxide ligands with alcohol or other rhenium alkoxides. This reaction cannot be used to prepare a hydroxycarbonyl derivative (cf. eq 9) since **16a** does not react with water in benzene or acetonitrile.

Discussion

Rhenium–Alkoxide and -Amide Bonding. The complexes reported herein are members of a growing family of low-valent rhenium–oxo compounds, including halide, carboxylate, pyridine, alkyl, and hydride compounds and dimeric derivatives. The alkoxide and amide complexes are of interest because the π-donor property of these ligands is a perturbation and a probe of the electronic structure of the molecules. We begin with a summary of a previous molecular orbital study of 1[3] and then introduce the alkoxide or amide π-donor interaction.

Rhenium–oxo compounds of the form $Re(O)X(RC{\equiv}CR)_2$ are best described as rhenium(III), d^4, and as obeying the 18-electron rule. The four rhenium electrons occupy d orbitals that are of δ symmetry with respect to the rhenium–oxo bond axis, the d_{xy} and $d_{x^2-y^2}$ orbitals (with the Re≡O vector taken as the z axis). The filled orbitals lie in the xy plane while the three d orbitals that have extension along the z axis (d_{xz}, d_{yz}, d_{z^2}) are to a first approximation empty. This unusual orbital arrangement is a result of the strong rhenium–oxygen triple bond.[3]

The rhenium–ligand π-interaction is favorable only when the ligand π-orbital overlaps with one of the empty rhenium d orbitals along the z axis. The π-donor orbital of alkoxide and amide ligands is a p orbital that is perpendicular to the ReOC or ReNHR plane so the ligands prefer to lie in the xy plane, with oxo–Re–O–C or oxo–Re–N–C torsion angles close to 90°. The interaction of the amide π-donor orbital with the rhenium d_{z^2} orbital is illustrated in B.

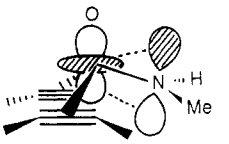

B

This is the orientation in **10a** on the basis of NMR spectra (see A above) and close to that observed in the structure of **7a** (∠O–Re–O–Ph = 69.2 (14)°, Figure 2). (A larger torsion angle in **7a** is apparently prevented by steric interactions between the phenyl group and an acetylene ligand.) The preference for this configuration is reinforced by an antibonding interaction that would occur if the ligand atoms were to lie in the xz plane (O–Re–O–C torsion angle = ~0 or 180°): the filled ligand p orbital would overlap with the filled rhenium d_{xy} orbital. Thus the amide and alkoxide ligands adopt a sterically crowded configuration in order to maximize metal–ligand π-bonding.

The π-donor interaction not only determines the orientation of the alkoxide and amide ligands but also appears to slightly weaken the rhenium–oxo bonding. The Re≡O stretching frequencies decrease in the order halide (~980 cm^{-1}) > alkoxide (~965 cm^{-1}) > amide (~940 cm^{-1}). This is consistent with the suggestion above that the alkoxide and amide π-donate into rhenium d orbitals along the z axis that are primarily involved in rhenium–oxo bonding. This is not, however, a strong enough interaction to cause a significant lengthening of the rhenium–oxo distance (1.697 (3) Å in **1a** and 1.712 (13) Å in **7a**). Rhenium–acetylene π-bonding does not appear to be affected since the ^{13}C chemical shifts of the acetylenic carbons[24] are very similar in **1a**, **2a**, **7a**, and **10a** (average values δ 140, 149, 148, and 146, respectively).

Ligand Exchange Reactions. The closely related pyridine complexes $[Re(O)(RC{\equiv}CR)_2py]^+$ have been shown to undergo ligand exchange reactions by an associative mechanism involving front-side attack at the tetrahedral rhenium center with retention of configuration.[7] The inequivalence of the acetylene substituents in the NMR provides a probe of the stereochemistry at the rhenium. The acid-catalyzed alkoxide/alcohol exchange reported here also proceeds with retention of configuration, as evidenced by the acetylene substituents remaining distinct. Therefore this catalyzed exchange is believed to occur by an associative mechanism similar to that suggested for pyridine exchange.[7] The origin of the acid catalysis appears to be protonation at the alkoxide oxygen to give a coordinated alcohol, which is then easily substituted by free alcohol.

(21) Angelici, R. J. *Acc. Chem. Res.* **1972**, *5*, 335–341. Bao, Q.-B.; Rheingold, A. L.; Brill, T. B. *Organometallics* **1986**, *5*, 2259–2265. Tasi, M.; Palyi, G. *Ibid.* **1985**, *4*, 1523–8. Bianchini, C.; Masi, D.; Meli, A.; Sabat, M. *Ibid.* **1986**, *5*, 1670–5. Vitagliano, A. *J. Organomet. Chem.* **1974**, *81*, 261.

(22) Bryndza, H. E.; Kretchmar, S. A.; Tulip, T. H. *J. Chem. Soc., Chem. Commun.* **1985**, 977–8. Bryndza, H. E. *Organometallics* **1985**, *4*, 1686-7.

(23) Rees, W. M.; Atwood, J. D. *Organometallics* **1985**, *4*, 402–4. Rees, W. M.; Churchill, M. R.; Fettinger, J. C.; Atwood, J. D. *Ibid.* **1985**, *4*, 2179–2185.

(24) ^{13}C chemical shifts of acetylenic carbon atoms are a sensitive measure of metal–acetylene π bonding: Templeton, J. L.; Ward, B. C. *J. Am. Chem. Soc.* **1980**, *102*, 3288–3290. Templeton, J. L.; Ward, B. C.; Chen, G. J.-J.; McDonald, J. W.; Newton, W. E. *Inorg. Chem.* **1981**, *20*, 1248–1253.

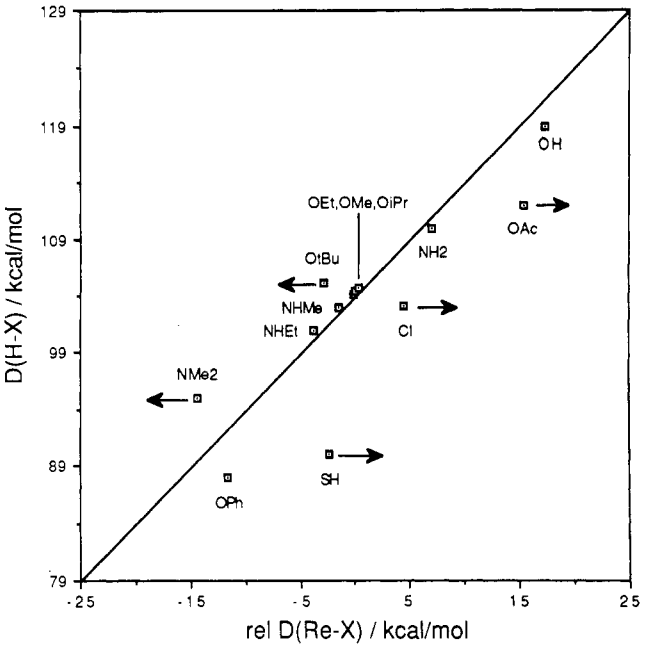

Figure 3. Plot of H–X bond strengths vs relative Re–X bond strengths in kcal/mol. Data taken from Table III, with Re–OEt assigned a relative bond strength of 0. A line with an arbitrary slope of 1 has been drawn through this point. The data for Re–OAc, Re–Cl, and Re–SH are minimum values and that for Re–O-*t*-Bu and Re–NMe_2 are maximum values, as indicated by the arrows.

While the data are most consistent with an associative process, a dissociative mechanism cannot be conclusively ruled out. As noted by a reviewer, protonation should also facilitate dissociation of an alcohol ligand. However, a dissociative mechanism would require that a three-coordinate intermediate, $[Re(O)(RC{\equiv}CR)_2]^+$, be stereochemically rigid on the time scale of ligand exchange. Ligand dissociation was not observed in the previous study for sterically crowded pyridines such as 2,6-lutidine.[7]

By analogy with the acid-catalyzed and pyridine exchange reactions, an associative pathway is reasonable for the uncatalyzed ligand exchange reactions in Scheme I (as illustrated below).

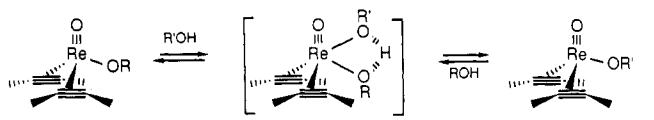

In this case, however, the NMR of the acetylene substituents is not informative because these reactions are slower than the NMR time scale. A similar associative mechanism can be envisioned for the exchange of alkoxide ligands between two rhenium centers.[25] While a dissociative mechanism involving an alkoxide/rhenium ion pair is possible, the formation of charged species seems unlikely in benzene solution, particularly given the lack of reaction of **3a** with CO_2 and its very slow reaction with CH_3I.

The ligand exchange reactions are in essence the exchange of one Re–X bond for another and one H–X bond for another (eq 11). Bryndza, Bercaw, and co-workers

$$\text{Re–X} + \text{H–X}' \rightleftharpoons \text{Re–X}' + \text{H–X} \qquad (11)$$

have recently used solution equilibrium data of this type to obtain estimates of relative metal–ligand bond strengths.[26] They concluded that the differences among

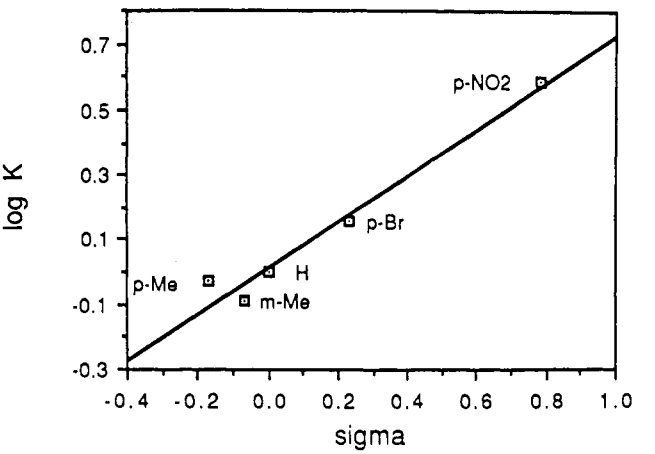

Figure 4. Hammet σ–ρ plot of log (K_{eq}) for the exchange of substituted phenols with Re(O)(OPh)(MeC≡CMe)$_2$ (**7a**).

metal–X bond energies are usually equal to the differences among the corresponding H–X bond energies.

A similar analysis in this system yields much the same conclusion that M–X bond energies parallel the values for H–X (Figure 3). In fact this conclusion follows directly from the observation of ligand exchange equilibria, since equilibrium constants between 0.01 and 100 yield small free energy differences ($|\Delta G°| < 2.7$ kcal/mol). It is only necessary to assume that heats of solution and sublimation are relatively constant within the system, which is supported by the facile sublimation of all the compounds at 40–70 °C and by the agreement between equilibrium constants measured in CD_2Cl_2, $CDCl_3$, and C_6D_6 solutions. The fact that neither *t*-BuOH nor $HNMe_2$ will displace EtOH from **3a** is presumably due to steric factors, and the stronger binding of SH and Cl groups compared to first-row ligands is attributed to hard/soft characteristics. These types of exceptions were noted in the previous study as well.[26]

It is interesting that acetate and to a lesser extent phenoxide bind more strongly to rhenium than the correlation would predict. The fact that these are the least basic of the first-row anions in this study suggests that bond strengths may be related to basicity in addition to homolytic bond strengths. Equilibria involving substituted phenols (Figure 4) support this correlation, since a linear Hammett σ–ρ plot is found, with a ρ value of $+0.71 \pm 0.06$. We have been unable to locate bond strengths for these phenols to determine if the equilibrium constants also parallel O–H bond strengths.

Carbon Monoxide Insertion. Two types of mechanisms are well established for the net insertion of CO into metal–alkoxide bonds: a true insertion involving an carbonyl–alkoxy intermediate has been established for the carbonylation of (dppe)Pt(OMe)X,[22] and an alternative pathway involving alkoxide dissociation and subsequent nucleophilic attack at a coordinated CO has been observed in reactions of $Ir(OR)(CO)(PPh_3)_2$.[23] The available evidence, which is not conclusive, suggests that the carbonylation of rhenium alkoxides proceeds by CO insertion into the Re–OR bond (as illustrated).

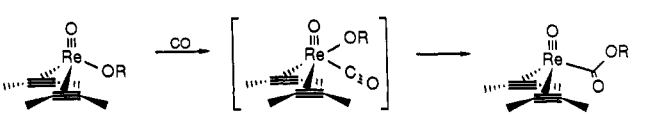

A carbonyl–alkoxy intermediate has not been observed (by

(25) For other examples of this type of transition state, see ref 18 and: Garrou, P. E. *Adv. Organomet. Chem.* **1984**, *23*, 95; Lubben, T. V.; Wolczanski, P. T. *J. Am. Chem. Soc.* **1987**, *109*, 424–435.

(26) Bryndza, H. E.; Fong, L. K.; Paciello, R. A.; Tam, W.; Bercaw, J. E. *J. Am. Chem. Soc.* **1987**, *109*, 1444–1456.

NMR at −80 °C), but an associative mechanism has precedent in the associative nature of the ligand exchange reactions. In contrast, alkoxide dissociation from the rhenium–oxo fragment seems unlikely. The reaction of **3a** with CO is only a factor of 2 faster in CH_2Cl_2 than in benzene, suggesting that ions are not involved (although the reaction could proceed through a tight ion pair). As mentioned above, the very slow reactions of **3a** with CO_2 and CH_3I argue against the presence of ionic ethoxide.

A test of the intramolecularity of the reaction via a crossover experiment, such as carbonylation of a mixture of **2a** and **3b**, is not possible because of the exchange of alkoxide ligands (eq 6). However, the fact that carbonylation of **3a** in the presence of *t*-BuOH gives **16a** with only a trace of the butoxycarbonyl derivative (~5%) (eq 12)

$$\underset{\textbf{3a}}{Re(O)(OEt)(MeC{\equiv}CMe)_2} + CO + t\text{-}BuOH \rightarrow Re(O)[C(O)OEt](MeC{\equiv}CMe)_2 \quad (12)$$
$$\textbf{16a}$$

suggests that an EtO^- ion is not an intermediate. A rhenium/ethoxide ion pair would have been expected to rapidly equilibrate with *t*-BuOH and yield a mixture of ethoxycarbonyl and *tert*-butoxycarbonyl products. Trapping of the ion pair by CO is unlikely to be faster than reaction with *tert*-BuOH given the low concentration of CO in solution.

Attempts to prepare the cationic carbonyl complex $[Re(O)(CO)(MeC{\equiv}CMe)_2]^+$ that might be attacked by an alkoxide have resulted in complete decomposition. For instance removal of the iodide ligand from **1a** in the presence of CO yields hexamethylbenzene and rhenium carbonyl complex(es) (eq 13). The oxo–carbonyl complex is presumably an intermediate in this reaction but is not stable (in contrast to a recently reported tungsten–oxo–carbonyl compound[27]).

$$\underset{\textbf{1a}}{Re(O)I(MeC{\equiv}CMe)_2} + TlPF_6 + CO \rightarrow TlI + C_6Me_6 + Re(CO)_x \ldots \quad (13)$$

Conclusions. Rhenium(III)–oxo–alkoxide compounds are readily prepared by metathesis of the rhenium–oxo–iodide **1** by thallium alkoxides. These complexes are significantly more reactive than the analogous alkyl[13] and halide[3] derivatives of the $Re(O)(RC{\equiv}CR)_2$ fragment. The alkoxide complexes decompose at less than 100 °C by a number of pathways including β-hydrogen elimination. They react with carbon monoxide to give alkoxycarbonyl products, probably by CO insertion into the Re–OR bond. Ligand exchange reactions with alcohols, amines, acids, and H_2S are observed, with equilibria being established within minutes at ambient temperatures. Amide and hydrosulfide complexes have been prepared by this route. As in the related cationic pyridine derivatives,[7] ligand exchange seems to proceed by an associative mechanism involving front-side attack at the tetrahedral rhenium center.

Spectroscopic studies and the X-ray crystal structure of the phenoxide derivative **7a** indicate that the alkoxide and amide ligands have a sterically unfavorable conformation. This structure is preferred for an electronic reason: to allow ligand π-donation to the rhenium center and minimize antibonding π-interactions.

Experimental Section

All reactions and preparations were performed under nitrogen using standard vacuum line techniques; sublimations were performed under dynamic vacuum (~10^{-2} mmHg). Benzene, pentane, acetonitrile, and toluene were vacuum transferred from CaH_2; methylene chloride, alcohols and deuteriated solvents were transferred from activated 4-Å sieves. NMR spectra were recorded on Varian CFT-20 and VXR-300 (^1H and ^{13}C) and Bruker CXP-200 and WM-500 spectrometers, in C_6D_6 solvent unless otherwise indicated, and are reported as chemical shift (multiplicity, coupling constant in Hz). IR spectra were obtained as Nujol mulls (unless otherwise indicated) by using a Perkin-Elmer 283 spectrometer. Mass spectra were recorded on a Hewlett-Packard 5985 GC/MS, using the direct inlet method with a 70-eV ionizing radiation (M^+ and base peak reported). Elemental analyses were performed by Canadian Microanalytical Service Ltd., Vancouver, British Columbia, or by Galbraith Laboratories, Knoxville, TN. Accurate elemental analyses have not been possible to obtain for compounds **2–5** because these solids decompose in sealed ampules within 2 days at 25 °C. Molecular weight determinations (MW) were done by the Signer Method based on differential vapor pressure osmometry.[28]

Thallium reagents (toxic and slightly light sensitive) were obtained from TlOEt (Strem) by metathesis with excess ROH, using either benzene or alcohol as solvent,[10] e.g.: TlOEt (1.02 g, 4.10 mmol) and MeOH (10 mL) were stirred at 25 °C for 15 min and white TlOMe (0.75 g, 77%) was filtered off, washed with methanol, and dried in vacuo. $TlOSiMe_3$ was prepared following a procedure for $NaOSiMe_3$[29] by using TlOEt in place of sodium metal. Anhydrous liquid ammonia was subjected to at least three freeze–pump–thaw cycles before vacuum transfer. Complexes **1**, **15a**, and $ReO(OAc)(MeC{\equiv}CMe)_2$ have been previously reported;[3] compounds **12** is described in ref 9, **13** in ref 13, and **14** in ref 8.

$ReO(OMe)(MeC{\equiv}CMe)_2$ (2a). Following the procedure for **3a**, 0.40 g (0.92 mmol) of **1a**, and 0.22 g (0.94 mmol) of TlOMe gave 0.19 g (60%) of pale yellow-green **2a**. IR: 1763 vw, 1160, 1066, 1031, 962 vs. 624, 532 s cm^{-1}. ^1H NMR: δ 4.99 (s OCH_3), 2.41 (q, 1), 2.37 (q, 1, $CH_3C{\equiv}CCH'_3$). ^{13}C NMR: δ 154.1 (s), 144.4 (s, $MeC{\equiv}C'Me$), 68.6 (q, 138, OCH_3), 16.3 (q, 129), 10.3 (q, 129, $CH_3C{\equiv}CC'H_3$). MS: *m/z* 342, 292.

$ReO(OMe)(EtC{\equiv}CEt)_2$ (2b). As for **3b**, **2b** (0.28 g, 80%) was obtained as a bright yellow-green oil from 0.43 g (0.88 mmol) of **1b** and 0.21 g (0.89 mmol) of TlOMe. **2b** sublimes at 45 °C. IR: 1805 vw, 1752 w, 1141 w, 1061, 1031, 969 vs. 940, 532 cm^{-1}. ^1H NMR: δ 4.98 (s, OCH_3), 3.05 (m, 2 H), 2.99 (m, 4 H), 2.83 (m, 2 H, $MeCHH'C{\equiv}CCH''H'''Me$), 1.16 (t, 8), 1.13 (t, 7, $CH_3CH_2C{\equiv}CCH_2CH'_3$). ^{13}C NMR: δ 157.4 (s), 148.4 (s, $EtC{\equiv}C'Et$), 68.5 (q, 138, OCH_3), 26.0 (t, 129), 20.2 (t, 130, $MeCH_2C{\equiv}CC'H_2Me$), 14.4 (q, 127, $CH_3CH_2C{\equiv}CCH_2C'H_3$). MS: *m/z* 398, 260.

$ReO(OEt)(MeC{\equiv}CMe)_2$ (3a). A mixture of 1.57 g (3.60 mmol) of **1a**, 0.90 g (3.61 mmol) of TlOEt, and 25 mL of CH_2Cl_2 was warmed from −80 °C and stirred at room temperature for 30 min. The solvent was replaced by 30 mL of pentane, TlI (1.20 g, 100%) was removed by filtration, and on pumping away the solvent an oil and eventually solids were obtained. The solid was sublimed at 33 °C to give 0.95 g (75%) of **3a** as pale yellow-green crystals. IR: 1818 vw, 1765 w, 1154, 1095, 1047 s, 964 vs (ν(ReO); $\nu(Re^{18}O)$ (from **1a**-^{18}O) = 916 cm^{-1}), 899, 626, 602 cm^{-1}. ^1H NMR: δ 5.07 (q, 7, OCH_2Me), 2.44 (q, 1), 2.38 (q, 1, $CH_3C{\equiv}CCH'_3$), 1.59 (t, 7, OCH_2CH_3). ^{13}C NMR: δ 154.0 (s), 144.0 (s, $MeC{\equiv}C'Me$), 73.9 (t, 139, OCH_2Me), 20.8 (q, 127, OCH_2CH_3), 16.3 (q, 129), 10.0 (q, 129, $CH_3C{\equiv}CC'H_3$). MS: *m/z* 356, 274. MW (CH_2Cl_2): calcd, 356; found, 412.

$ReO(OEt)(EtC{\equiv}CEt)_2$ (3b). Following the procedure for **3a**, 0.65 g (1.3 mmol) of **1b** and 0.34 g (1.4 mmol) of TlOEt gave 0.47 g (87%) of **3b** as a yellow oil. **3b** can be sublimed (as an oil) at 45 °C. IR: 1807 w, 1755, 1146, 1095, 1049 s, 968 vs, 941, 608 cm^{-1}. ^1H NMR: δ 5.04 (q, 7, OCH_2Me), 3.07 (m, 2 H), 2.99 (m, 4 H), 2.85 (m, 2 H), $MeCHH'C{\equiv}CCH''H'''Me$), 1.59 (t, 7, OCH_2CH_3), 1.18 (t, 8), 1.15 (t, 8 $CH_3CH_2C{\equiv}CH_2CH'_3$). ^{13}C NMR: δ 157.4 (s), 148.0 (s, $EtC{\equiv}C'Et$), 74.0 (t, 138, OCH_2Me), 20.8 (q, 125, OCH_2CH_3), 26.0 (t, 127), 20.1 (t, 124, $MeCH_2C{\equiv}CC'H_2Me$), 14.4 (q, 127, $CH_3CH_2C{\equiv}CCH_2C'H_3$). MS: *m/z* 412, 260.

(27) Su, F.-M.; Cooper, C.; Geib, S. J.; Rheingold, A. L.; Mayer, J. M. *J. Am. Chem. Soc.* **1986**, *108*, 3545–3547. Bryan, J. C.; Geib, S. J.; Rheingold, A. L.; Mayer, J. M. *J. Am. Chem. Soc.* **1987**, *109*, 2826–2828.

(28) Clark, E. P. *Ind. Eng. Chem., Anal. Ed.* **1941**, *13*, 820–1.

(29) Belmonte, P. A.; Own, Z.-Y. *J. Am. Chem. Soc.* **1984**, *106*, 7493–6.

ReO(OEt)(*t*-BuC≡CH)$_2$ (3c). Following the procedure for **3a**, 1.52 g (3.08 mmol) of **1c** and 0.77 g (3.09 mmol) of TlOEt gave **3c** (1.16 g, 91%) as a yellow oil. IR (neat): 3096, 1706, 1680, 1236 s, 1211, 1202, 1150, 1091 s, 1048 s, 974 vs, 964 s, sh, 904 s, 768 s, 613, 600, 569 cm^{-1}. ^{1}H NMR: δ 9.90 (s), 8.42 (s, *t*-BuC≡C*H*), 4.96 (q, 7, OCH_2Me), 1.45 (t, 7, OCH$_2$CH_3), 1.55 (s), 1.34 (s, (CH_3)$_3$CC≡CH).

ReO(O-*i*-Pr)(MeC≡CMe)$_2$ (4a). Following the procedure for **3a**, 0.55 g (1.3 mmol) of **1a** and 0.35 g (1.3 mmol) TlO-*i*-Pr gave 0.32 g (69%) of **4a** as a pale yellow-green crystalline solid. IR: 1816 w, 1763, 1354, 1309, 1159, 1116 s, 1043, 975–955 vs, 621 sh, 610 cm^{-1}. ^{1}H NMR: δ 5.23 (sep, 6, OC*H*Me$_2$), 2.44 (q, 1), 2.37 (q, 1, CH_3C≡CC*H*′$_3$), 1.60 (d, 6, OCH(CH_3)$_2$). ^{13}C NMR: δ 153.9 (s), 143.5 (s, MeC≡*C*′Me), 76.3 (d, 139, O*C*HMe$_2$), 27.1 (q, 125, OCH(*C*H$_3$)$_2$), 16.3 (q, 129), 9.6 (q, 129, *C*H$_3$C≡C*C*′H$_3$). MS: *m/z* 370, 274.

ReO(O-*t*-Bu)(MeC≡CMe)$_2$ (5a). Following the procedure for **3a**, 0.70 g (1.6 mmol) of **1a** and 0.45 g (1.6 mmol) of TlO-*t*-Bu gave 0.46 g (74%) of yellow-green **5a**. IR: 1753 w, 1356, 1176 s, 1157, 1042, 967 vs, 938 s, 625, 579 cm^{-1}. ^{1}H NMR: δ 2.45 (s), 2.43 (s, CH_3C≡CC*H*′$_3$), 1.70 (s, OC(CH_3)$_3$). ^{13}C{^{1}H} NMR (CDCl$_3$): δ 156.3, 145.6 (MeC≡*C*′Me), 74.6 (O*C*Me$_3$), 32.8 (OC(*C*H$_3$)$_3$), 17.0, 10.9 (*C*H$_3$C≡C*C*′H$_3$). MS: *m/z* 384, 274.

ReO(OSiMe$_3$)(MeC≡CMe)$_2$ (6a). Following the procedure for **3a**, 0.46 g (1.0 mmol) of **1a** and 0.31 g (1.0 mmol) of TlOSiMe$_3$ gave 0.31 g (75%) of yellow-green **6a**. IR: 1791 w, 1782 w, 1359, 1252, 1240 vs, 1157, 1035, 990-935 vs, 832 vs, 624 cm^{-1}. ^{1}H NMR: δ 2.39 (s), 2.38 (s, CH_3C≡CC*H*′$_3$), 0.51 (s, OSi(CH_3)$_3$). ^{13}C NMR: δ 155.1 (s), 143.3 (s, MeC≡*C*′Me), 16.8 (q, 129), 9.6 (q, 129, *C*H$_3$C≡C*C*′H$_3$), 3.7 (q, 117, OSi(*C*H$_3$)$_3$). MS: *m/z* 400, 274. Anal. Calcd for C$_{11}$H$_{21}$O$_2$SiRe: C, 33.07; H, 5.30. Found: C, 32.90; H, 5.20.

ReO(OPh)(MeC≡CMe)$_2$ (7a). Following the procedure for **3a**, 0.17 g (0.38 mmol) of **1a** and 0.12 g (0.39 mmol) of TlOPh gave 0.11 g (70%) of yellow-green **7a** from cold pentane. **7a** sublimes at 60 °C. IR: 1815 vw, 1774 vw, 1589 s, 1484 vs, 1241 vs, 1160, 1145, 1045, 968, 958 s, 846 s, 765 s, 692 s, 625, 496 cm^{-1}. ^{1}H NMR: δ 7.38 (d, 8), 7.25 (t, 8), 6.89 (t, 8, OC$_6$*H*$_5$ (o, m, p)), 2.37 (q, 1), 2.05 (q, 1, CH_3C≡CC*H*′$_3$). ^{13}C{^{1}H} NMR (CDCl$_3$): δ 167.8, 128.9, 121.6, 119.8 (O*C*$_6$H$_5$), 153.5, 142.9 (MeC≡*C*′Me), 16.8, 8.8 (*C*H$_3$C≡C*C*′H$_3$). MS: *m/z* 404, 350. Anal. Calcd for C$_{14}$H$_{17}$O$_2$Re: C, 41.68; H, 4.25. Found: C, 41.51; H, 4.15.

ReO(OPh)(*t*-BuC≡CH)$_2$ (7c). A solution of **1c** (0.10 g, 0.21 mmol) and TlOPh (0.06 g, 0.21 mmol) in 20 mL of CH_2Cl_2 was stirred at room temperature for 0.5 h, filtered, and concentrated to about 1 mL. Addition of 15 mL of pentane and cooling to −80 °C gave analytically pure pale green **7c** (0.06 g, 61%). IR: 3082 w, 1707 w, 1676, 1585, 1228 vs, br, 1156, 984, 966 vs, 908, 766 s, 694 s, 624, 597, 566 cm^{-1}. ^{1}H NMR: δ 9.98 (s), 7.93 (s, *t*-BuC≡C*H*), 7.21 (m, 4 H), 6.88 (t, 7, 1 H, OC$_6$*H*$_5$), 1.51 (s), 1.15 (s, (CH_3)$_3$CC≡CH). ^{13}C NMR: δ 169.7 (s), 164.2 (s, *t*-Bu*C*≡CH), 141.4 (d, 215), 123.7 (d, 216, *t*-BuC≡*C*H), 168.2 (s), 129.4 (d, 156), 122.6 (d, 154), 120.9 (d, 159, O*C*$_6$H$_5$), 38.4 (s), 35.7 (s, Me$_3$*C*C≡CH), 31.2 (q, 127), 31.1 (q, 127, (*C*H$_3$)$_3$CC≡CH). Anal. Calcd for C$_{18}$H$_{25}$O$_2$Re: C, 47.04; H, 5.48. Found: C, 46.81; H, 5.51.

ReO(OCH$_2$CH=CH$_2$)(MeC≡CMe)$_2$ (8a). Following the procedure for **3a**, 0.65 g (1.5 mmol) of **1a** and 0.39 g (1.5 mmol) of TlOCH$_2$CH=CH$_2$ gave pale yellow-green crystalline **8a** (0.42 g, 77%). IR: 3093 w, 3006, 1817 w, 1763, 1643, 1160 s, 1107, 1046 vs, br, 998 vs, 963 vs, br, 910 s, 628, 617, 560 cm^{-1}. ^{1}H NMR: δ 6.30 (ddt, 17, 10, 4, OCH$_2$C*H*=CH$_2$), 5.58 (m, OCH_2CH=CH$_2$), 5.51 (dq, 17, 2, OCH$_2$CH=C*H*H′), 5.21 (dq, 10, 2, OCH$_2$CH=CH*H*′), 2.41 (q, 1), 2.36 (q, 1, CH_3C≡CC*H*′$_3$). ^{13}C NMR: δ 153.7 (s), 144.1 (s, MeC≡*C*′Me), 141.1 (d, 152, OCH$_2$*C*H=CH$_2$), 112.9 (t, 156, OCH$_2$CH=*C*H$_2$), 79.9 (t, 138, OCH_2CH=CH$_2$), 16.5 (q, 129), 10.1 (q, 130, *C*H$_3$C≡C*C*′H$_3$). MS: *m/z* 368, 274.

ReO(NH$_2$)(MeC≡CMe)$_2$ (9a). Complex **5a** (0.63 g, 1.6 mmol) was stirred in 20 mL of benzene under 1 atm of NH_3 for 0.5 h at room temperature. The volatiles were pumped off, the residue was redissolved in 20 mL of benzene and stirred under NH_3 for another hour. After filtration and solvent removal, sublimation at 40 °C yielded 0.30 g (55%) of beige-white **9a**. IR: 3463 sh, 3371 sh, 1784, 1553, 1159, 1044, 945 vs, 623 cm^{-1}. ^{1}H NMR: δ 3.99 (br s, NH_2), 2.46 (q, 1), 2.13 (q, 1, CH_3C≡CC*H*′$_3$). ^{13}C NMR: δ 146.8 (s), 138.1 (s, MeC≡*C*′Me), 16.0 (q, 129), 6.5 (q, 129, *C*H$_3$C≡C*C*′H$_3$). Anal. Calcd for C$_8$H$_{14}$ONRe: C, 29.44; H, 4.32; N, 4.29. Found: C, 29.55; H, 4.34; N, 3.92. MW (CH_2Cl_2): calcd, 326; found, 312.

ReO(NHMe)(MeC≡CMe)$_2$ (10a). A solution of **5a** (0.42 g, 1.1 mmol) in 25 mL of benzene was stirred for 20 min under 1 atm of H_2NMe at room temperature. After filtration and removal of the solvent, sublimation at 40 °C gave 0.21 g (56%) of **10a** as a pale green crystalline solid. IR: 3486 sh, 1796 vw, 1763 w, 1160, 1094, 1046, 962, 936 vs, 630, 619, 549 cm^{-1}. ^{1}H NMR: δ 4.71 (br s, N*H*Me), 3.95 (d, 7, NH(CH_3)), 2.49 (s), 2.20 (s, CH_3C≡CC*H*′$_3$). The high-field acetylene resonance is broad at 25 °C but sharp at 80 °C. ^{13}C NMR: δ 148.6 (br s), 142.5 (vbr s, CH$_3$C≡*C*′CH$_3$), 46.4 (q, 133, NH(*C*H$_3$)), 15.7 (q, 128), 10.1 (br q, ~128, *C*H$_3$C≡*C*′H$_3$). Anal. Calcd for C$_9$H$_{16}$ONRe: C, 31.73; H, 4.74; N, 4.11. Found: C, 31.58; H, 4.70; N, 3.79. MW (CH_2Cl_2): calcd, 341; found, 420.

ReO(SH)(MeC≡CMe)$_2$ (11a). A solution of **3a** (0.44 g, 1.2 mmol) in 15 mL of benzene was stirred under 1 atm of H_2S for 1 h at room temperature. Removal of the volatiles yielded 0.38 g (90%) of **11a**: sublimation at 36 °C gave a colorless solid. IR: 2547 vw, 1806 w, 1788, 1157 s, 1039, 974 vs, 953 vs, 627, 381 cm^{-1}. ^{1}H NMR: δ 2.67 (s, S*H*), 2.38 (q, 1), 2.35 (q, 1, CH_3C≡CC*H*′$_3$). ^{13}C NMR: δ 142.0 (s), 137.4 (s, MeC≡*C*′Me), 15.3 (q, 130), 8.9 (q, 130, *C*H$_3$C≡C*C*′H$_3$). MS: *m/z* 344, 288. Anal. Calcd for C$_8$H$_{13}$OSRe: C, 27.98; H, 3.82. Found: C, 28.06; H, 3.84. MW (CH_2Cl_2): calcd, 343; found, 306.

ReO[C(O)OEt](MeC≡CMe)$_2$ (16a). A solution of **3a** (0.18 g, 0.51 mmol) in 5 mL of C_6H_6 was stirred under 1 atm of CO at 50 °C for 22 h, the volatiles were removed, and the residue was recrystallized from pentane. Sublimation at 45 °C gave analytically pure off-white **16a** (0.08 g, 43%). IR: 1798 w, 1662 s, 1157, 1081 s, 1048, 964 vs, 648, 628 cm^{-1}. ^{1}H NMR: δ 4.37 (q, 7, OCH_2Me), 2.52 (q, 1), 2.40 (q, 1, CH_3C≡CC*H*′$_3$), 1.13 (t, 7, OCH$_2$CH_3). ^{13}C{^{1}H} NMR: δ 204.0 (*C*(O)OEt), 141.0, 139.4 (MeC≡*C*′Me), 60.2 (O*C*H$_2$Me), 14.9 (OCH$_2$*C*H$_3$), 15.4, 12.8 (*C*H$_3$C≡C*C*′H$_3$). MS: *m/e* 384, 274. Anal. Calcd for C$_{11}$H$_{17}$O$_3$Re: C, 34.45; H, 4.47. Found: C, 34.24; H, 4.36.

ReO[C(N-*i*-Pr)OEt](MeC≡CMe)$_2$ (17a). CN-*i*-Pr (49 μL, 0.54 mmol, Strem) was added dropwise to a stirred solution of **3a** (0.18 g, 0.51 mmol) in 15 mL of C_6H_6. After for $^1/_2$ h, the benzene was replaced by 15 mL of pentane. Filtration, pentane removal from the filtrate, and sublimation at 55 °C gave light beige **17a** (0.08 g, 38%). IR: 1801 vw, 1791 w, 1612 vs, 1358, 1354, 1167, 1142, 1096 s, 1041, 976, 965, 951 s, 629, 599 cm^{-1}. ^{1}H NMR: δ 4.29 (q, 7, OCH_2Me), 4.10 (sept. 6, NC*H*Me$_2$), 2.51 (s), 2.47 (s, CH_3C≡CC*H*′$_3$), 1.59 (d, 6, NCH(CH_3)$_2$), 0.95 (t, 7, OCH$_2$CH_3). ^{13}C NMR: δ 186.4 (s, *C*(N-*i*-Pr)OEt), 142.9 (s), 139.8 (s, MeC≡*C*′Me), 62.7 (t, 146, O*C*H$_2$Me), 56.7 (d, 132, N*C*HMe$_2$), 26.0 (q, 125, NCH(*C*H$_3$)$_2$), 15.3 (q, 124, OCH$_2$*C*H$_3$), 15.4 (q, 129), 13.4 (q, 129, *C*H$_3$C≡C*C*′H$_3$). MS: *m/z* 425, 371. Anal. Calcd for C$_{14}$H$_{24}$O$_2$NRe: C, 39.61; H, 5.70; N, 3.30. Found: C, 39.37; H, 5.73; N, 3.20.

ReO(NHEt)(MeC≡CMe)$_2$ was generated in equilibrium with **3a** by condensing H_2NEt (50 mmHg in 100 mL, 0.27 mmol) into an NMR tube containing 0.05 g (0.14 mmol) of **3a** and C_6D_6 to give a volume of 0.50 mL and sealing the tube with a torch. ^{1}H NMR: δ 4.78 (br m, N*H*Et), 4.15 (m, NHCH_2Me), 2.51 (q, 1), 2.23 (br s, sharp at 50 °C, CH_3C≡CC*H*′$_3$), 1.31 (t, 7, NHCH$_2$CH_3).

ReO(NMe$_2$)(MeC≡CMe$_2$) was generated in equilibrium with **5a** by condensing 0.12 mmol of $NHMe_2$ into an NMR tube containing 0.01 g (0.02 mmol) of **5a** and C_6D_6 to give a volume of 0.50 mL and the tube sealed with a torch. ^{1}H NMR: δ 3.78 (s, N(CH_3)$_2$), 2.50 (q, 1), 2.33 (q, 1, CH_3C≡CC*H*′$_3$).

Reaction of **3a** with $CDCl_3$ (eq 4): An NMR tube containing **3a** (30 mg, 0.07 mmol) and 0.5 mL of $CDCl_3$ was evacuated and sealed with a torch. After 13 h at 70 °C, an NMR spectrum indicated that **3a** had been consumed and showed **15a** (60% yield based on **3a**), $CHDCl_2$ (25%), and MeCHO (25%) as the only identifiable products.

Reaction of **3a** with **2b** (eq 6): An NMR tube containing **3a** (30 mg, 0.07 mmol) and **2b** (30 mg, 0.07 mmol) in 0.5 mL of C_6D_6 was evacuated and sealed with a torch. Equilibrium, with equimolar amounts of **2a**, **2b**, **3a**, and **3b**, was established within 24 h (by NMR).

Reaction of **12a** with CO (eq 9): CO (1 atm) was admitted into a 50-mL glass bomb containing 20 mL of a 0.02 M solution of **12a** in C_6D_6. The yellow-green solution turned orange after stirring

Table IV. Summary of X-ray Diffraction Data

complex	$Re(O)(OC_6H_5)(CH_3C{\equiv}CCH_3)_2$ (**7a**)
formula	$C_{14}H_{17}O_2Re$
fw	403.49
cryst dimens	0.40 × 0.33 × 0.20 mm
radiatn	Mo Kα, λ = 0.7107 Å from graphite monochromator
temp, °C	23 ± 2
space group	$Pna2_1$
a, Å	18.620 (7)
b, Å	7.2389 (9)
c, Å	10.552 (3)
V, Å^3	1422.3 (7)
Z	4
ρ_{calcd}, g/cm^3	1.88
μ, cm^{-1}	86.5
θ limits, deg	2–25
transmissn factors	0.604–0.999; av 0.803
total no. of reflectns	2887
data $I > 3\sigma$	987
final no. of variables	83
R	0.044
R_ω	0.044
goodness of fit	1.12

for 4 days, and water droplets appeared on the walls of the bomb. The volatiles were removed to yield 0.22 g (79%) of **14a** (identified by NMR).

Reaction of **16a** with MeOH (eq 10): An NMR tube containing **16a** (30 mg, 0.07 mmol), MeOH (5.0 μL, 0.12 mmol), and C_6D_6 (0.5 mL) was evacuated and sealed with a torch. The reaction gave 80% conversion to $Re(O)[C(O)OMe](MeC{\equiv}CMe)_2$ after 10 h at 70 °C (by NMR).

Equilibrium Constants. The equilibrium constants given in Table III were determined in benzene-d_6 solution at 22 ± 2 °C by ^{1}H NMR integration. Equilibrium was attained within minutes, and several spectra were used to obtain an average K_{eq} and an estimate of the uncertainty involved. Several equilibria were examined in both directions with good agreement.

X-ray Structure of $Re(O)(OC_6H_5)(CH_3C{\equiv}CCH_3)_2$ (7a). A yellow crystal of **7a**, grown by slow evaporation of a pentane solution, was mounted on a glass fiber roughly along a. Preliminary photographic examination and data collection were performed on an Enraf-Nonius CAD4 diffractometer. Cell constants and an orientation matrix were obtained by least-squares refinement, using the setting angles of 25 reflections in the range $9 < \theta < 21°$. Good crystal quality was suggested by measuring ω scans of several intense reflections; the peak widths at half-height were ~0.4°. Final parameters are shown in Table IV, as are other crystallographic data. Intensity data were collected by using θ–2θ scans. The scan rate was fixed at 2.8 °/min (in ω). The scan range was calculated as $\Delta\omega = 1.10 + 0.347 \tan\theta$ (ratio of peak counting time to background counting time = 2:1). The systematic absences ($h0l$, h odd; $0kl$, $k + l$ odd) suggest two possible space groups: $Pna2_1$ (No. 33) and $Pnam$ (No. 62). The data were scaled for linear decay (maximum correction 7.9%) and an empirical absorption correction based on a set of ψ-scans was applied. The data were averaged over $mm2$ symmetry, and the R factors for the averaging of 2791 reflections were 9.9% based on intensity and 6.7% based on F_o.

The Re atom position was revealed in a Patterson synthesis. The remaining atoms were located in succeeding difference fourier maps in space group $Pna2_1$. Hydrogen atom positions on the phenyl ring were calculated (C–H = 1.00 Å) and were added to the structure factor calculations without refinement. The structure was refined in full-matrix least-squares where the function minimized was $\sum w(|F_o| - |F_c|)^2$ with $w = 4F_o^2/\sigma^2_{F^2}$. The data were processed with a p value of 0.04 to down-weight intense reflections.[30] Scattering factors and anomalous dispersion terms were taken from the standard compilations.[31] The 987 reflections with $I > 3\sigma$ were used in the refinements. A final cycle of refinement with 83 parameters converged (largest parameter shift was 0.01σ) with unweighted and weighted R factors of $R = \sum||F_o| - |F_c||/\sum|F_o| = 0.044$ and $R_w = \sqrt{\sum w(F_o - F_c)^2/\sum wF_o^2} = 0.046$, and a goodness of fit $S = \sqrt{\sum w(F_o - F_c)^2/(n - \nu)} = 1.17$. One reflection with an abnormally large residual was deleted and refinement continued; final cycle: $R = 0.044$, $R_\omega = 0.044$, $S = 1.12$. The three highest peaks in the final difference Fourier map with heights of 1.2–1.8 e/Å^3, and the eight lowest negative peaks with heights of −0.92 to −1.4 e/Å^3 are close to the rhenium atom. All calculations were performed on a MICRO-VAX computer using the SDP/VAX program supplied by the Enraf-Nonius Corp. Positional and equivalent isotropic thermal parameters of the non-hydrogen atoms are listed in Table I; selected bond lengths and angles are given in Table II. A complete table of bond lengths and angles and tables of anisotropic thermal parameters, idealized hydrogen atom positions, and observed and calculated structure factor amplitudes are available as supplementary material.

Acknowledgment. We thank B. D. Santarsiero, S. C. Critchlow, and V. Schomaker for their assistance with the X-ray crystallography. This work was supported by an M. J. Murdock Charitable Trust Grant of the Research Corp., by the Chevron Research Co., by the National Science Foundation (CHE-8617965), and by the donors of the Petroleum Research Fund, administered by the American Chemical Society. We also acknowledge support of X-ray equipment from the National Science Foundation (CHE-8617023) and the Graduate School Research Fund of the University of Washington (PHS grant RR-07096).

Supplementary Material Available: Tables of bond lengths and angles, anisotropic thermal parameters, and idealized hydrogen atom positions for $Re(O)(OPh)(MeC{\equiv}CMe)_2$ (**7a**) (2 pages); a table of observed and calculated structure factor amplitudes for **7a** (5 pages). Ordering information is given on any current masthead page.

(30) Corfield, P. W. R.; Doedens, R. J.; Ibers, J. A. *Inorg. Chem.* **1967**, *6*, 197–204.
(31) *International Tables of X-Ray Crystallography*; Kynoch: Birmingham, England, 1974; Vol. IV, Tables 2-2B, 2.3.1.